STRESS-STRAIN ANALYSIS OF TIRE UNDER VARIATIONS OF SLIP ANGLES USING FINITE ELEMENT METHOD

Mohammad Rahim Nami, Mohammad Sarabian, Ali Farazi

Department of Mechanical Engineering, Shiraz University, Shiraz, 71348-51154, Iran

m.sarabian@shirazu.ac.ir

ABSTRACT

The tire moving on different surfaces is subjected to different stresses and strains. In order to predict stress behavior of tire and its durability, the amount of these stresses and strains should be determined. Slip angles are among the factors which influence stresses and strains of the tire. In this study a three-dimensional model of tire was constructed and the stated angles were enforced to consider their effects. Then the amount of displacements, strains and stresses in each situation, inside or on the concerned structure were calculated in the model for different Slip angles, the vertical and lateral forces were obtained from the experimental data of Kagayama-Kuwahara and Smith works and applied in to the tire model. The results show that increase in Slip angles will lead to a drastic increase in asymmetrical stresses and strains which are the most important in tire heterogeneous wearing life and decreasing its durability. Therefore, it is necessary to make initial adjustment to have the least possible Slip angles while the tire is moving on road.

Key words: Stress,Strain,Tyre,Slip Angles

Corresponding Author: Mohammad Rahim Nami

INTRODUCTION

The first concern in mechanics of composite materials is to evaluate the effective mechanical properties or effective formant and basic principals which has been the subject of many research in studying composite materials [1]. Basically, the formulation of such a problem leads to investigating and solving of a complex problem with difficult boundary conditions that no analytical solution has been accomplished yet [2]. As mentioned before, finite element problems can be formulated by assuming unknown strains or stresses[3]. The strain method is able to result in relatively accurate solutions for displacements while the stresses computed by this method are less precise which is mostly seen in regions undergoing stress concentration or with severe stress

changes[4]. The method of finite element formulating according to stresses or loads, on the other hand offers accurate solutions for the stresses; therefore this method is employed in problems in which interlayer stresses are more important [5]. The first step in analysis of composite materials using finite element method is to evaluate the stress-strain relations[6]. Figure 1 shows a layer of a composite material with fiber orientation

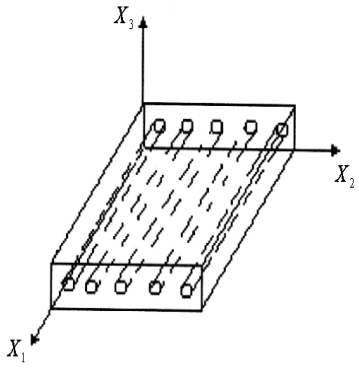

Figure 1: a layer of a composite material [7]

Here, assuming homogeneous and orthotropic layers, directions 1, 2, and 3 are known as the principal ones which are coincident with the fiber orientation [8].

1-Finite Element Meshing of the problem

In finite element method, the desired region/area is divided to smaller parts called elements which are connected to each other at certain points called nodes. The magnitudes of displacements of nodes are fundamental unknowns in finite element method [9]. The displacements in elements are then evaluated in based on the magnitudes of node displacements using shape functions[10].

Finite element analysis is carried out using different elements and different meshes. The mesh must be so fine that it can model composite materials and their fibers properly[11].

We can define different layers in an element and interlayer stresses are computed for that element layers[12]. The multi-layer structure, with or without considering shear deformations, may also be simulated by using a shell. In some of these cases no distinction is made between the layers and thus, the interlayer stresses are not computed. The analysis may be linear or non-linear[13]. In these entire cases finite element method is the most useful one for analyzing composite structures[14]. Finite element method is formulated in mechanical analysis of bodies using the rules of continuum mechanics[15].

In problems using shell elements, the displacements and their first and second derivatives should be continuous functions. In other words, the continuity conditions are satisfied at the element boundaries[16].

The solutions are always singular in linear problems while this does not apply to non-linear problems; i.e. if convergence condition is fulfilled and an answer is obtained, it's not necessarily the right solution[17]. Accurate definition of the boundary conditions and constraints of the problem, specific and smooth application of the load and solving the problem through small stages, have significant effects on obtaining the accurate solution[18].

2- Tire Modeling

2-1- Geometrical Modeling of the Tire

In this work a radial tire of model P150/82R13 is investigated. The tire parts geometrical coordinates required for computer modeling are listed. The tire consists of treads, walls, 2 layer of carcass and 4 layers of Beriker[19].

Each of the four layers of the Beriker is similarly defined by 5 points in the XY plane and only 3 points because of symmetry. The method for plotting the shells of the Beriker is the same as that of the carcass. Also each layer of the Beriker is meshed by 532 elements[20].

In order to model the tread and the wall, the partition in between the outer layer of the tire and the last layer of the carcass and Beriker has been considered and the area surrounded by these points shows the treads and the wall cross section in XY plane Shown in fig 2. Revolution of this cross section about the x-axis results in a volume representing the solid part of the treads and the wall[21]. The tire has been modeled with different numbers of sectors including four, six, and eight. The final modeling has been carried out in the optimum state which has been found to be 5 sectors of 72˚with lower calculation duration and more accurate results. The treads and the wall are modeled by 37860 elements[22].

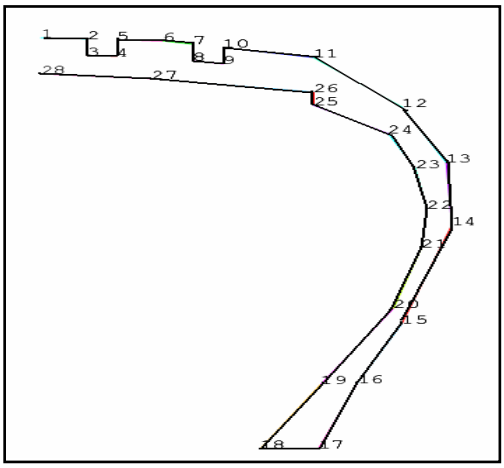

Fig.2. Model of a half cross section of the treads and the wall

In order to enhance the calculations accuracy, the lower sector of the tire which is in contact with the ground has been meshed with finer elements and more number of nodes in the way that it consists of 13039 elements while the other four sectors are meshed with 6205 elements.

In order to define a uniform tire composed of treads, wall, and layers of carcass and Beriker, one should define contact elements for the parts in contact so as to prevent them from interference. For instance, the first and second carcass or the fourth Beriker towards the lower layer of the treads are defined as contact elements.

The ground is defined as a rigid volume and the elements of the sector of tire which touches the ground are chosen to be contact elements[23].

Shown in figure 3 are the parts of the tire modeled and are meshed in figure 4.

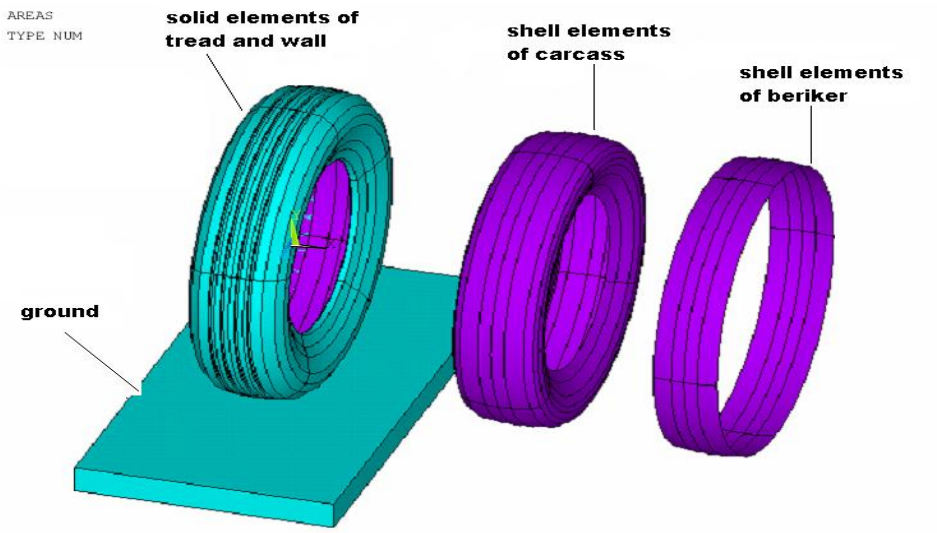

Fig.3. Solid and shell elements representing the tire and the ground

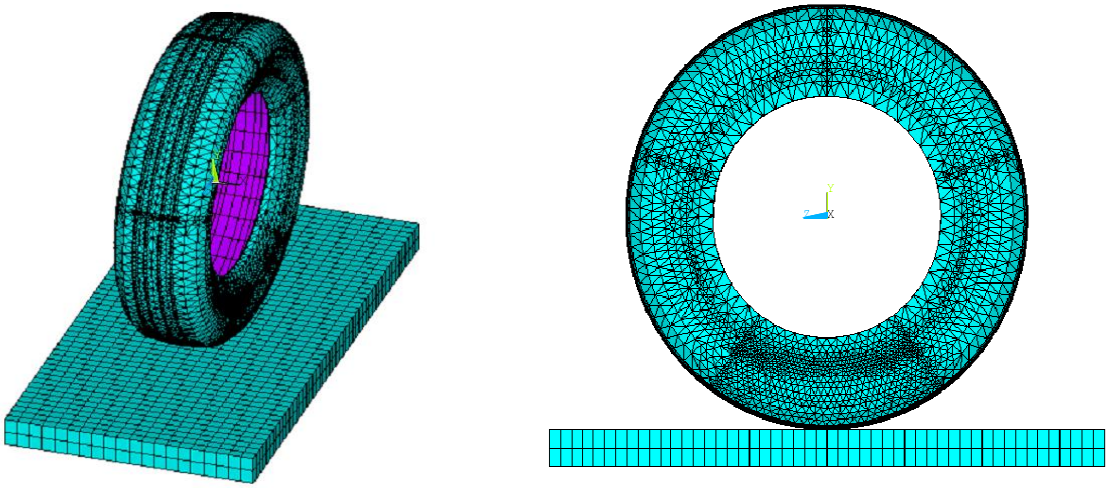

Fig 4. Meshed tire and ground prepared for load application

2-2. Boundary Conditions and Load Application

Accurate defining of loads magnitudes and their distribution across the tire is one of the most difficult issues in tire analysis; thus for simplification the following assumptions have been made:

1.Bead bundle is assumed to be stationary in this analysis and its motion is stopped using constraints.

2.In this F.E. simulation the wall and treads of the tire are modeled with rigid volumetric elements and the parts of carcass and Beriker are modeled with shell elements which are coupled to those of the wall and treads in their corresponding nodes.

3.Internal air pressure is defined by applying pressure to the inner surface of the first layer of carcass.

4.The effect of slip angle has been considered by rotating the tire about y axis until the direction of motion of the tire which has been along the z axis makes an angle of α with this axis.

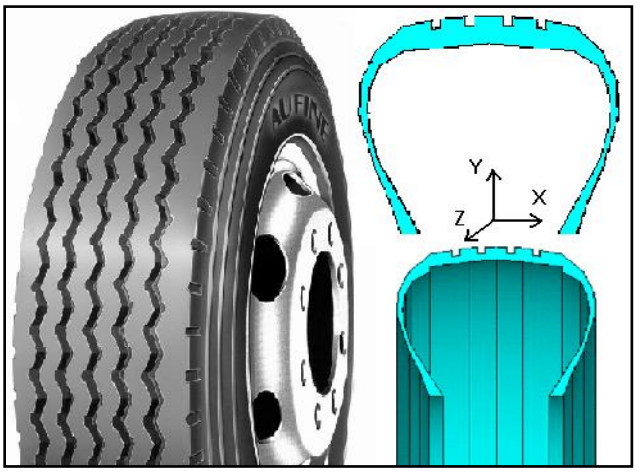

Fig 5. The tire and its cross section[24]

3- Results

3-1. Model Validation

Represented in figures 5-1 are lateral force vs. normal force and slip angles which have been obtained experimentally. Exerting the normal force for different simulated slip angles, the lateral force can be computed and compared with experimental results. Since the results agree, the primary modeling is valid and it can be expanded for further analysis including different slip angles and normal forces.

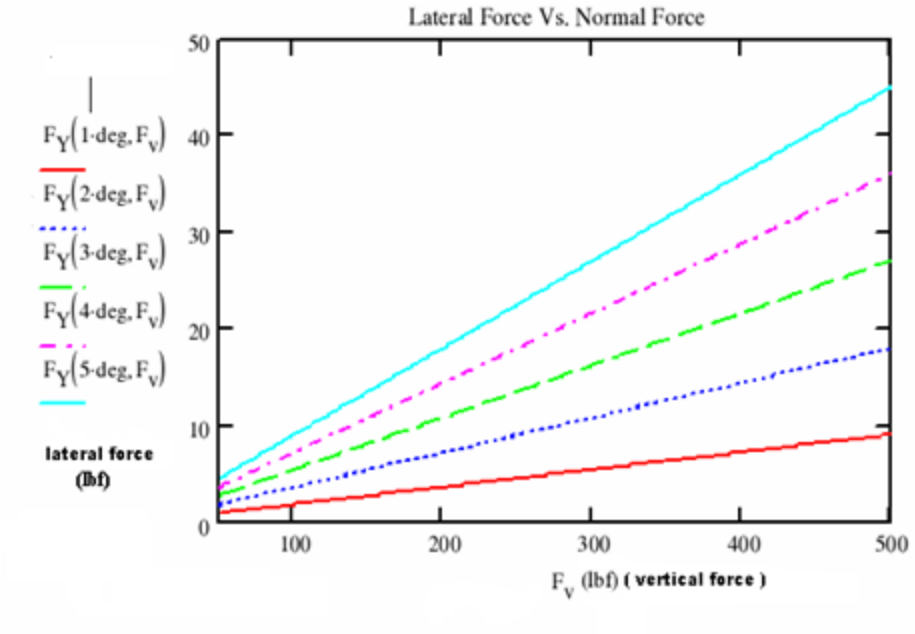

Fig. 5-1. Experimental plots on lateral force vs. normal force and slip angle[25]

For slip angles of 1, 3, and 6 degrees the magnitudes of normal and lateral forces in the contact area of tire and ground are determined and compared to experimental results in table 5-2 in order to estimate the error percentages.

Table 5-2. Comparison of experimental data and this work for slip angle

Slip angle (degree)	Vertical force (N)	Computed lateral force (N)	Measured lateral force (N)	Percentage error
1	818 /1	120/53	111 /3	8/3
3	820 /2	246/92	225 /5	9/5
6	821 /1	685/92	623	10/1

Since the obtained results agree with those of Smith, it has been found appropriate to use these results for model validation.

From tables 5-1 and 5-2 the errors made by the software are no more than 10.1 % which are obviously results of dissimilarity in conditions of the experiment from those considered in the software.

3-2. Results

Primarily the von-misses stress contour in the tire according to equation 3-35 represented by the software and displacement of the sector in touch with the ground are investigated for three cases of **a)** zero slip angle **b)** 1 degree slip angle.

3-2-1. Tire with zero slip angles

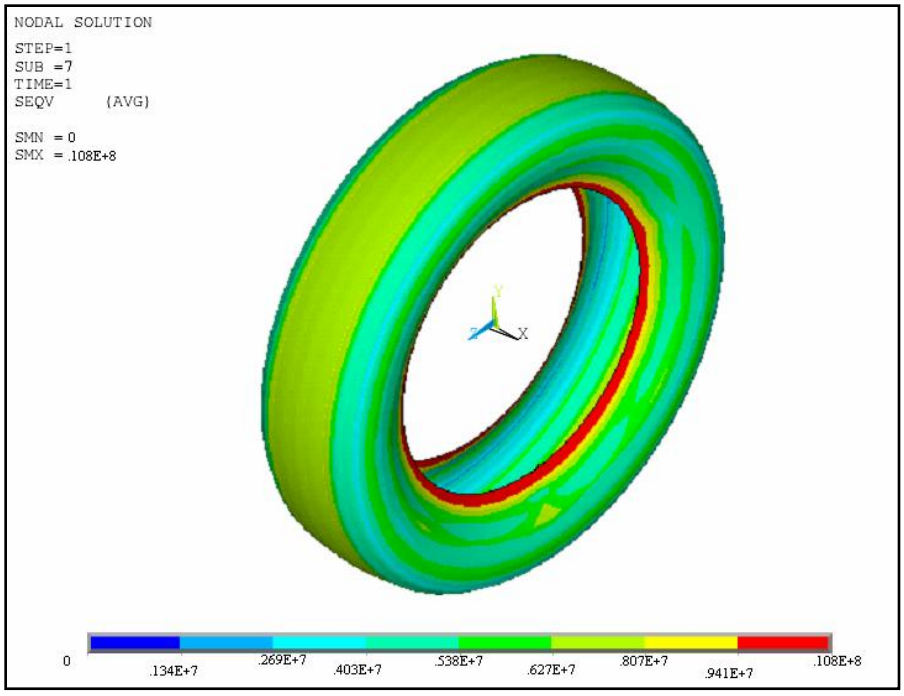

Fig.5.3. Von mises stress and its distribution in solid elements

As shown in fig.5.3, the maximum stress occurs in the wall of the tire as a consequence of its thinness relative to other parts. The maximum stress point is denoted in fig.5.8.

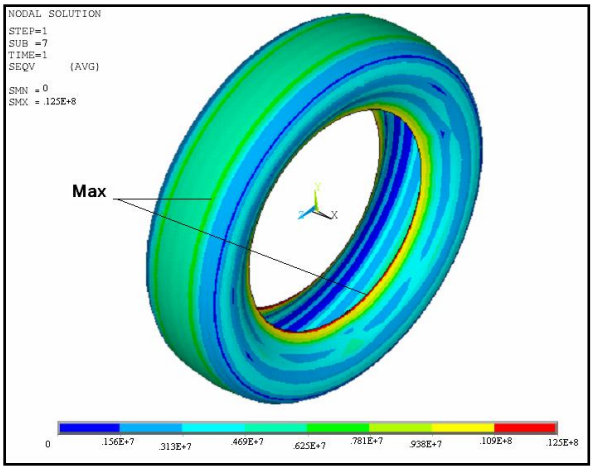

Fig. 5.4. Von mises stress and its distribution in shell elements of carcass's first laye

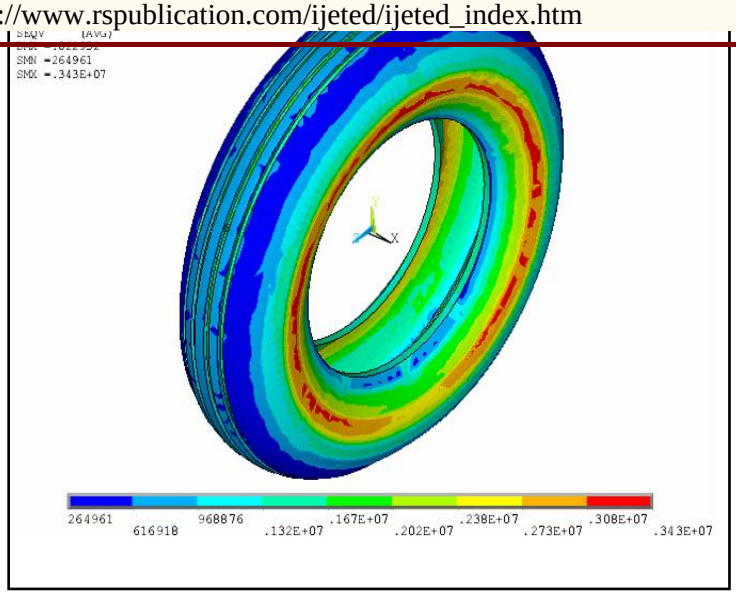

Fig. 5.5. Von mises stress and its distribution in shell elements of carcass's second layer

Considering figures 5.4 and 5.5 the maximum stress in layers of carcass, occurs at the junction with the Bead bundle and contact area with the Beriker.

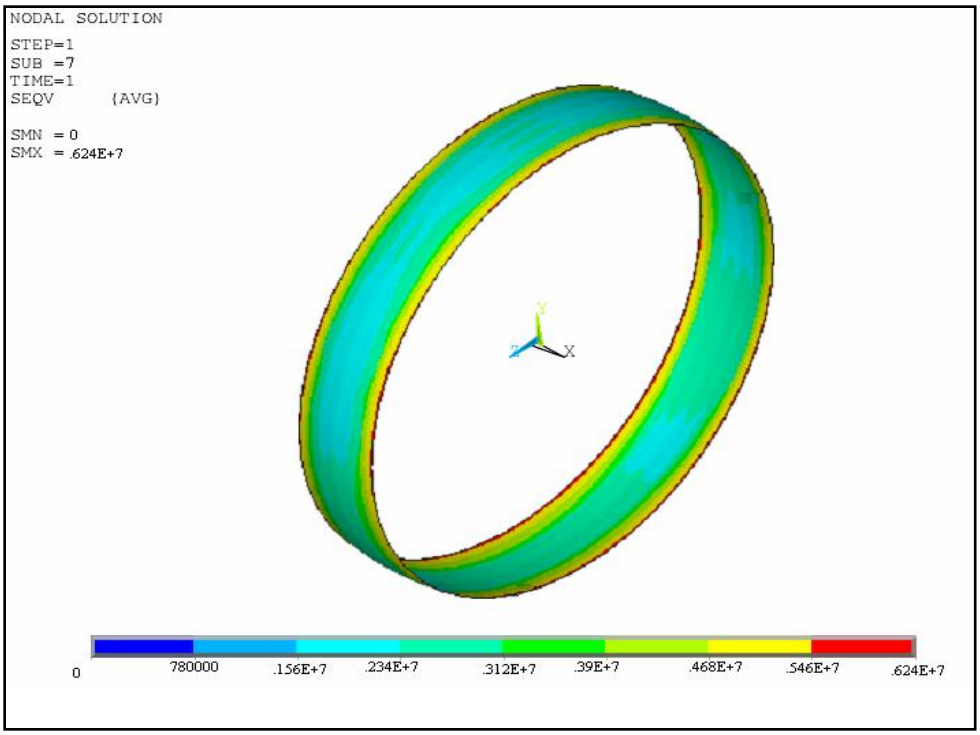

Fig. 5.6. Von mises stress and its distribution in shell elements of Beriker's first layer

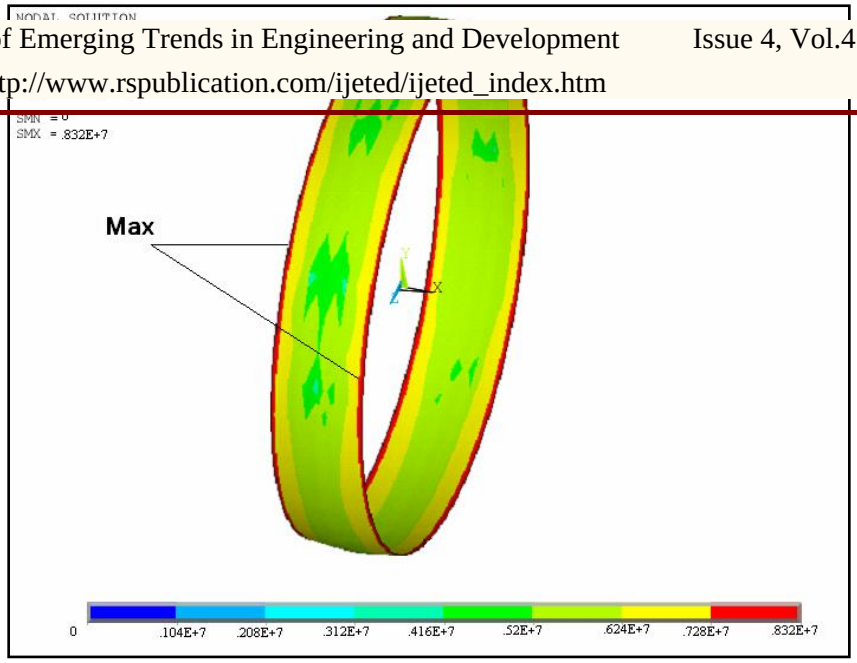

Fig. 5.7. Von mises stress and its distribution in shell elements of Beriker's third layer

Figures 5.6 and 5.7 show that in Berikers, the maximum stress occurs at the joint with the shoulders of the tire.

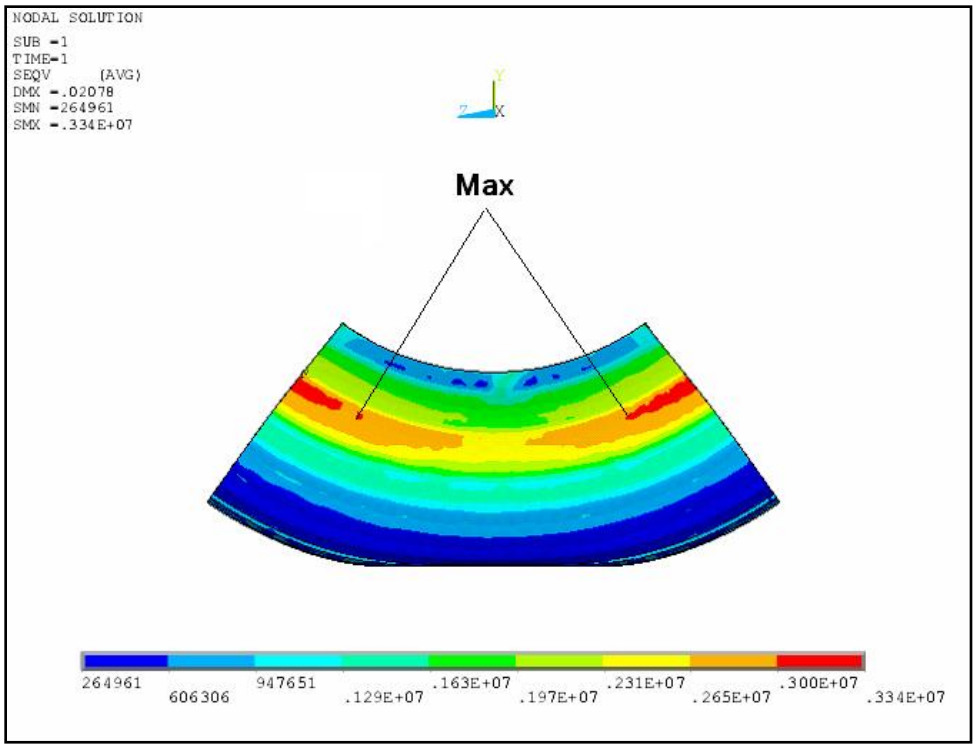

Fig. 5.8. Von mises stress and its distribution in solid elements of the tire's lower sector

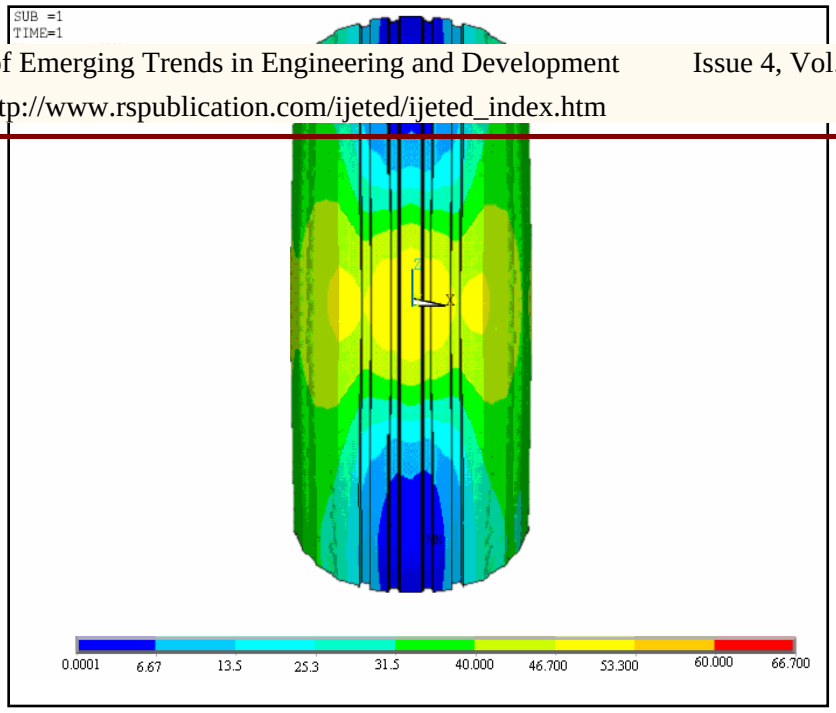

Fig. 5.9. Vertical strain and its distribution in solid elements of the tire's lower sector

As shown in figures 5.8 and 5.9, we have symmetric stresses and strains in the part of the tire contacting the ground surface in the condition of zero slip angle .In this case there exists less asymmetric wear and consequently the most lifetime for tire.

3.2.2. Tire with a 1˚ slip angle

Shown in fig.5.10 is the stress contour in a tire with 1˚ slip angle.

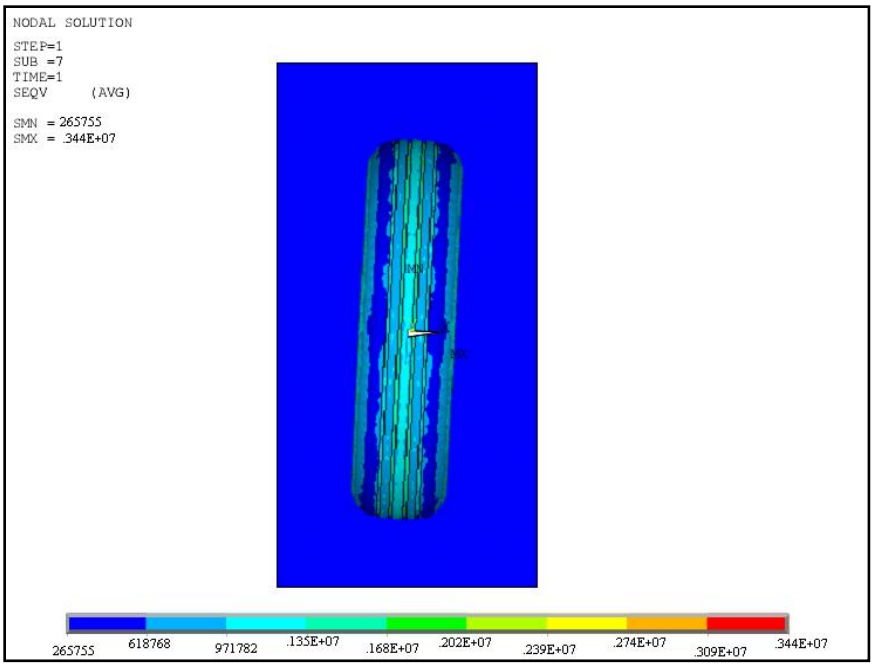

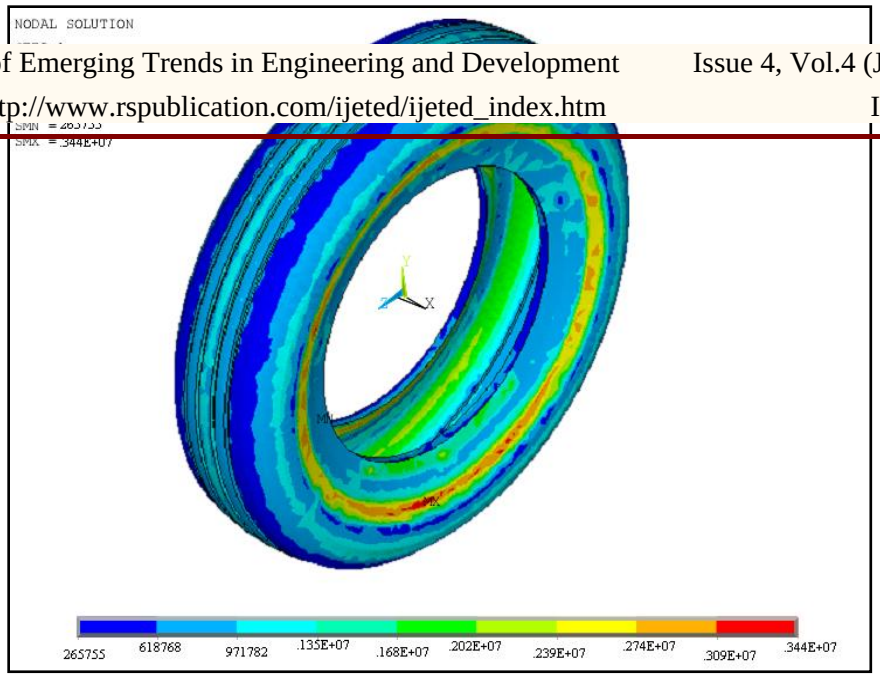

Fig. 5.10. Von mises stress distribution in of a tire with 1˚ slip angle

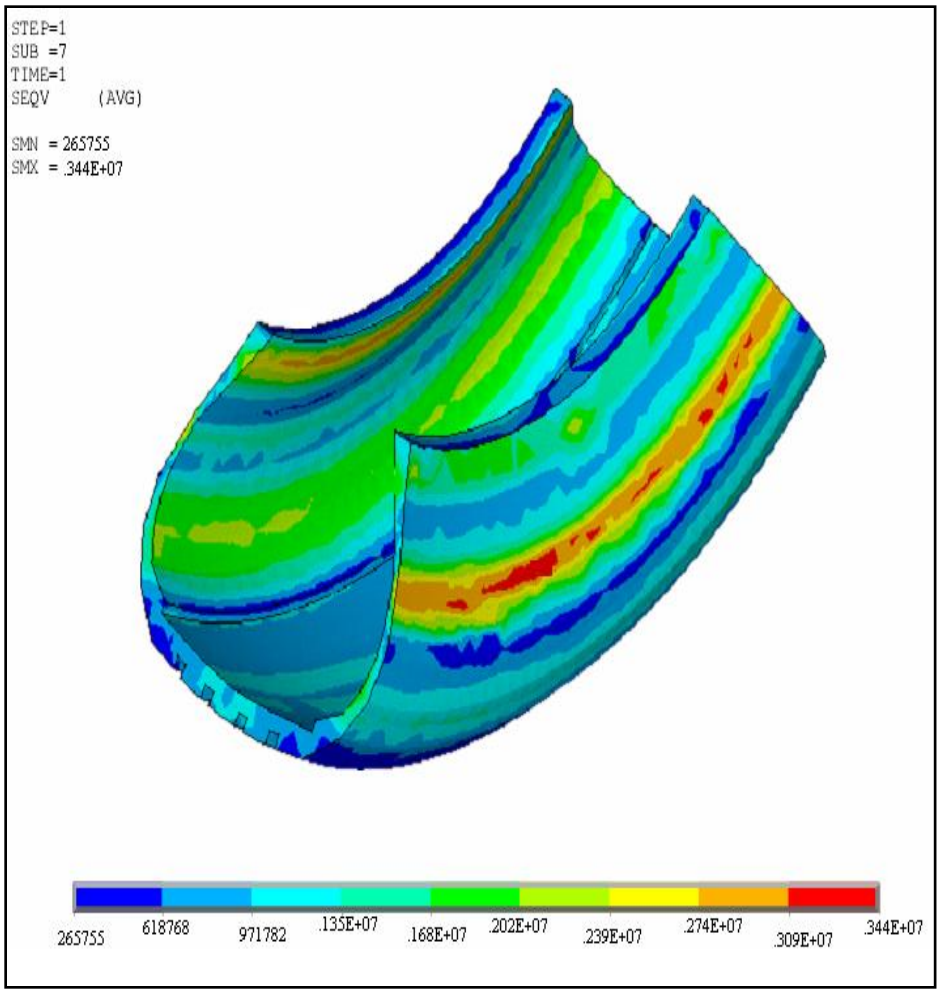

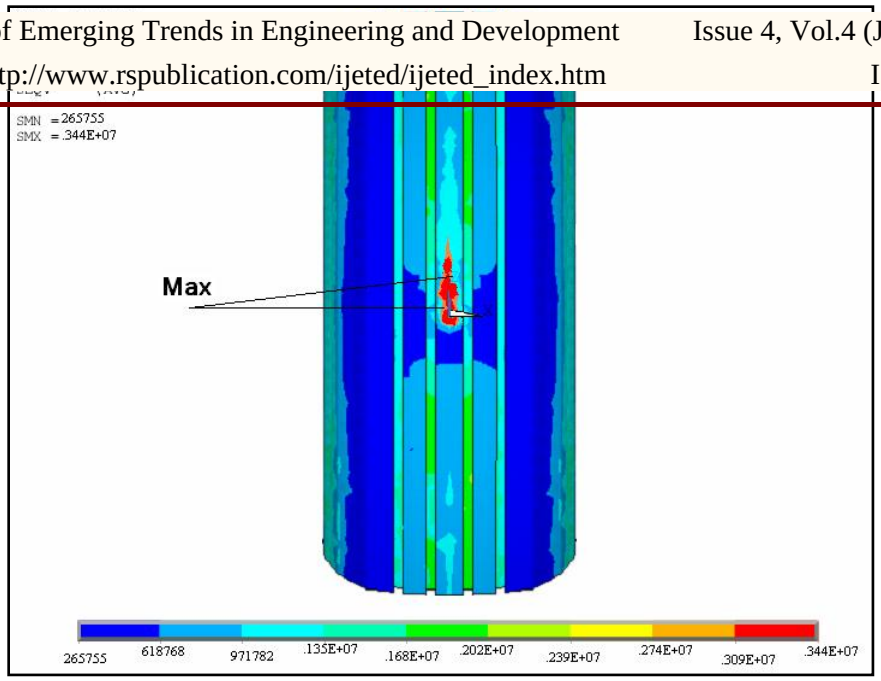

Fig. 5.11. Von mises stress distribution in lower sector of a tire with 1˚ slip angle

Fig. 5.11. shows the stress in lower sector of the tire and the contact condition of the tire with the ground with 1˚ slip angle. It's obvious that the stress is approximately symmetric with respect to the z-axis while the contact stress of the back half of the tire is considerably more than the frontal one's.

3.2.3. Stress Analysis in Contact Surface

Since it is one of the most important parameters in tire wear, here the contact surface is investigated. In order to accomplish this goal two main lines are defined, one across the surface area and another along the circumference of the tire. The stresses are inspected on these two lines for different slip angles. Fig. 5.12 shows the nodes and the shape of contact area for zero slip angle.

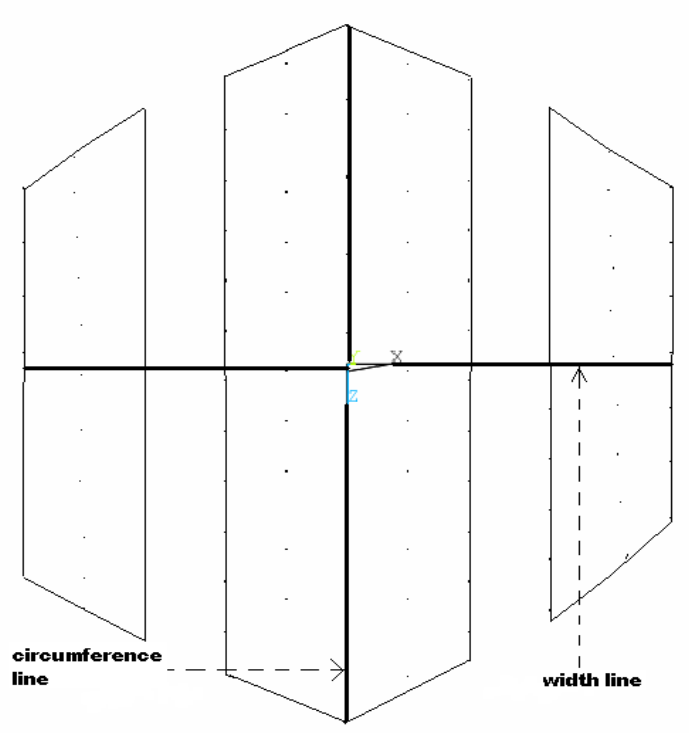

Fig. 5.12. Nodes and shape of the contact area for zero slip angle

3.2.3.1. Stress on the lateral line under different slip angles

Figure 5.13 shows the stress values on the lateral line for different slip angles of 0, 1, 3, and 6 degrees, in this situation the maximum stress occurs at the center of the lateral line and it increases in a cumulative manner as the slip angle rises.

In zero slip angle condition the maximum stress takes place at the edges of the middle tread. There is also a stress extreme happening at the center of this tread which is lower than the edges' in value. The stress distribution in slip angle conditions is almost similar to that of no slip angle situation except that the peak stress at the tread's center increases exponentially with increment of the slip angle in such a way that the stress magnitude at the center is significantly more than the stresses in the edges. The stress magnitude of the center of the tread grows more sharply until the slip angle of 3˚, but afterwards the growth is smoother.

In order to investigate the side treads more conveniently figures 5.13 and 5.14 are drawn.

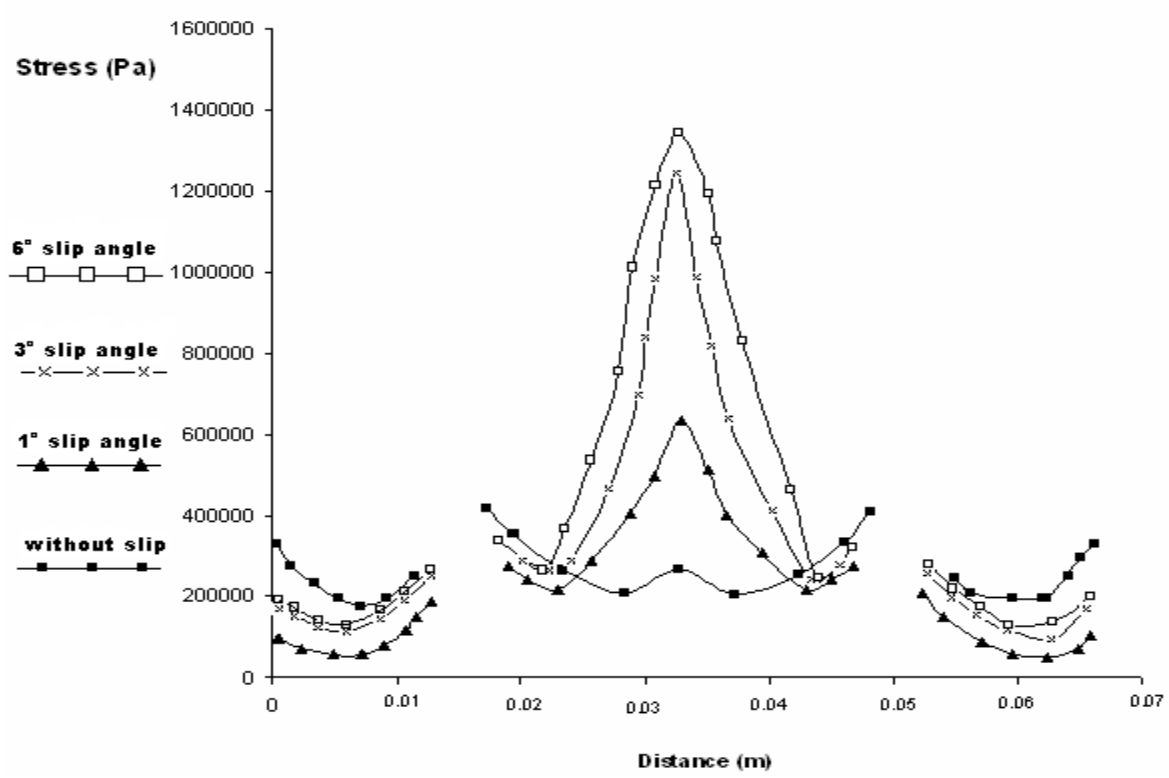

Fig. 5.13. Von mises stress on the lateral line for different slip angles

Fig. 5.14 gives a clearer image of the stress variation on the lateral line in the left tread for different slip angles. The left side of the diagram represents the outer edge and the right side shows the inner edge of the tread.

For no slip angle the stress is distributed in a way that the peak load occurs on the outer edge and reaches its minimum approximately at the center and continues a ascendant trend to the inner edge. This trend is different when there is a slip angle, as the maximum stress takes place on the inner edge and reaches a minimum at the center. As we move toward the outer edge, the stress traverses an ascendant trend.

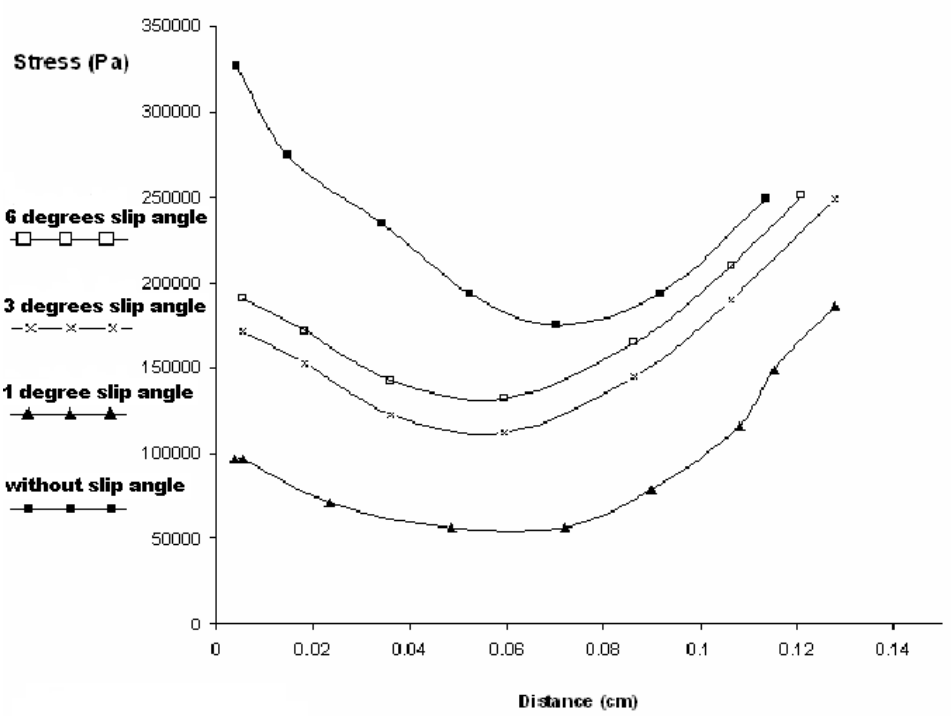

Fig. 5.14. Von mises stress on the lateral line for different slip angles in the left side tread

Fig. 5.15 shows the stress variations on the lateral line in the right tread for different slip angles more clearly. The right side represents the outer edge and the left side shows the inner edge of the tread. For zero slip angle the stress is distributed in a way that the maximum stress occurs in the outer edge and reaches its minimum almost at the center and continues an ascendant trend to the other edge.

This trend is different when there is a slip angle, as the maximum stress occurs in the inner edge and reaches a minimum value at the center and goes on in an ascendant manner to the outer edge. Fig. 5.16 shows the contact between the treads and ground for various slip angles in which few changes could be seen for different slip angles.

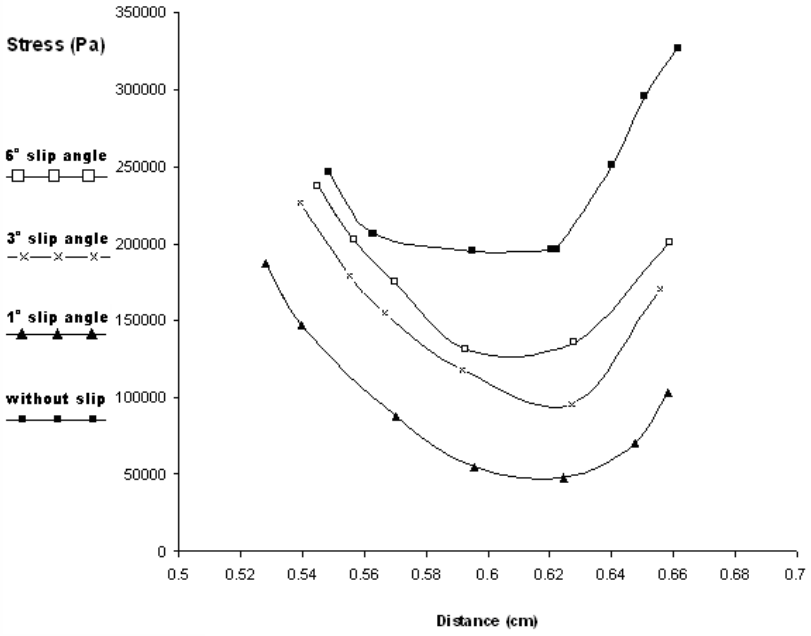

Fig. 5.15. Von mises stress on the lateral line for different slip angles in the right side tread

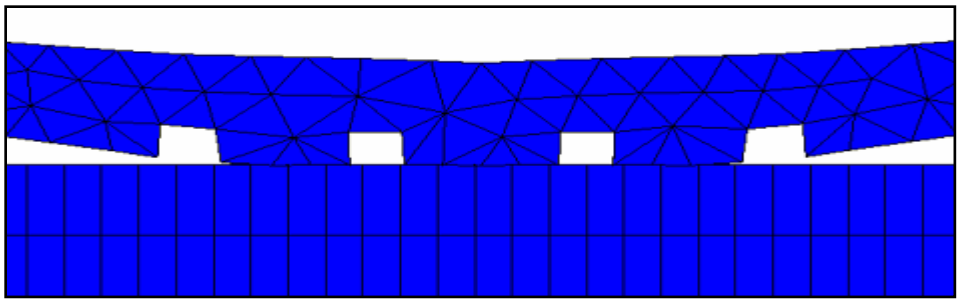

Fig. 5.16. Contact between the tread and ground for different slip angles

3.2.3.2. Stress on the peripheral line under different slip angles

Fig 5.17 shows the magnitude of the stress on the peripheral line for slip angles of 0, 1, 3, and 6 degrees. It's obvious from the figure that for slip angles of 1, 3, 6 degrees the peak stress takes place at a slight distance before the center of the peripheral line, unlike the no slip angle condition in which the maximum stress occurs at the center. This distance is due to the effect of the inflated tire. The stress changes on the circumferential line traverse an ascendant trend as the slip angle increases.

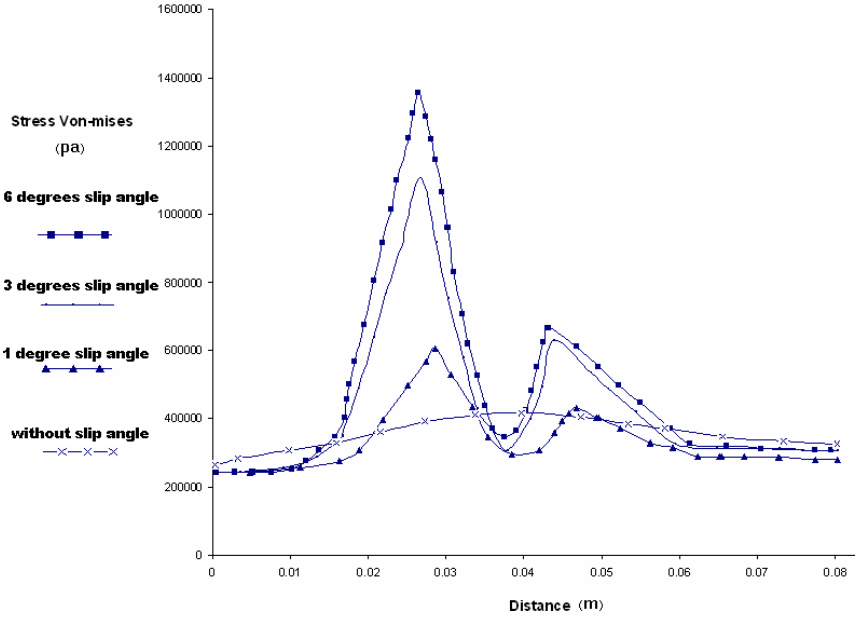

Fig. 5.17. Von mises stress on the peripheral line for different slip angles

3.2.4. The deformation of the tire cross section in contact with ground

An inflated tire which is loaded and is in contact with the ground, subjects to deformations in its different parts. Figures 5.18 show these changes in cross sections in different conditions.Fig. 5.18 shows the deformation of the tire due to loading for no-slip angle condition. As expected, this deformation is symmetrical.

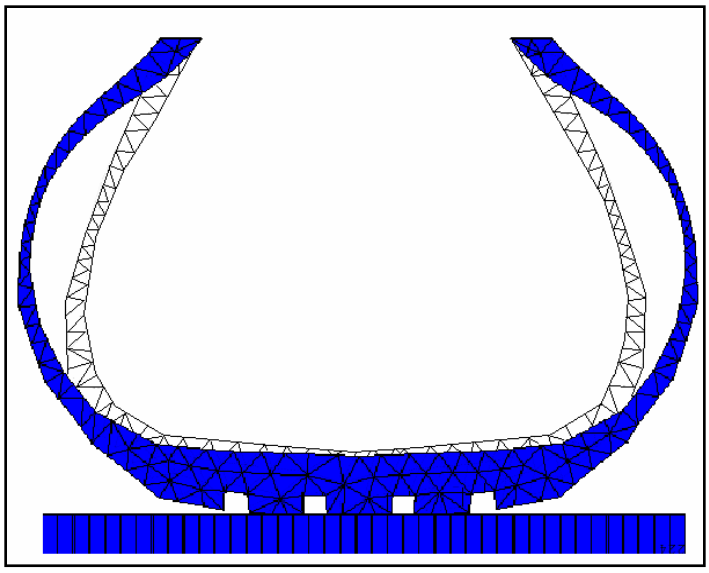

Fig. 5.18. The cross section of a tire in contact with the ground under no slip angle

CONCLUSION

Performing a 3D analysis of the tire using finite element method, one can obtain acceptable results while achieving more data and preventing the high expenses of an experimental approach in addition to higher speed and more ability of prediction[21]. Another advantage of non-linear solution of the problems on the other hand is to giving in results that are close to reality because of considering the effects of large deformations. As it was examined before, the lateral force produced because of slip angles may cause asymmetric wear and reduction in tire lifetime.Slip angles are caused only in turnings and steering[4]. Generally, this angle are considered as one important parameter in tire life[6]. All in all, we should prevent maximum contact stresses due to slip angles which are respectively exponentially and directly proportional by adjusting the suspension and steering system of the vehicle in order to avoid tire wear.

REFERENCES

[1] J. R. Cho , H. W. Leea, J. S. Sohna, G. J. Kimb, J. S. Woob,Numerical investigation of hydroplaning characteristics of three-dimensional patterned tire,European Journal of Mechanics A/Solids vol. 25, pp 914–926,2006.

[2] X. Yan, Y. Wang, X. Feng,Study for the endurance of radial truck tires with finite element modeling, Mathematics and Computers in Simulation vol. 59 pp. 471–488,2002.

[3] X. Feng, X. Yan, Y. Wei, X. Du, Analysis of extension propagation process of interface crack between belts of a radial tire using a finite element method, Applied Mathematical Modelling vol. 28 pp. 145–162,2004.

[4] A. Mohsenimanesh, S. M. Ward, M. D. Gilchrist, Stress analysis of a multi-laminated tractor tyre using non-linear 3D finite element analysis, Materials and Design vol. 30 pp. 1124–1132,2009.

[5] K. Hofstetter, C. Grohs, J. Eberhardsteiner, H. A. Mang, Sliding behaviour of simplified tire tread patterns investigated by means of FEM, Computers and Structures vol. 84 pp. 1151–1163,2006.

[6] Y. Waki, B. R. Mace, M. J. Brennan, Free and forced vibrations of a tyre using a wave/finite element approach, Journal of Sound and Vibration vol. 323 pp. 737–756,2009.

[7] J. R. Choa, J. H. Choia, W. S. Yooa, G. J. Kimb, J. S. Woob, Estimation of dry road braking distance considering frictional energy of patterned tires, Finite Elements in Analysis and Design vol. 42 pp. 1248 – 1257,2006.

[8] C. W. Fervers, Improved FEM simulation model for tire–soil interaction, Journal of Terramechanics vol. 41 pp. 87–100,2004.

[9] J. R. Cho, S. W. Shin, W. S. Yoo, Crown shape optimization for enhancing tire wear performance by ANN, Computers and Structures vol. 83 pp. 920–933,2005.

[10] J. Pelc, Towards realistic simulation of deformations and stresses in pneumatic tyres, Applied Mathematical Modelling vol. 31 pp. 530–540,2007.

[11] R. Merzouki, B. Ould-Bouamama, M. A. Djeziri , M. Bouteldja, Modelling and estimation of tire–road longitudinal impact efforts using bond graph approach, Mechatronics vol. 17 pp. 93–108,2007.

[12] F. Herna´ndez-Olivares, G. Barluenga, B. Parga-Landa, M. Bollati, B. Witoszek, Fatigue behaviour of recycled tyre rubber-filled concrete and its implications in the design of rigid pavements, Construction and Building Materials vol. 21 pp. 1918–1927,2007.

[13] A. H. ENGLAND, Finite Elastic Deformations of a Tyre Modelled as an Ideal Fibre-Reinforced Shell, Journal of Elasticity vol. 54 pp. 43–71, 1999.

[14] C. Schäfer, E. Finke, Shape optimisation by design of experiments and finite element methods—an application of steel wheels, Struct Multidisc Optim vol. 36 pp. 477–491, 2008.

[15] K. Akca, M. Cehreli, Biomechanical consequences of progressive marginal bone loss around oral implants: a finite element stress analysis, Med Bio Eng Comput vol. 44 pp .527–535, 2006.

[16] Q. Meng, Y. Huang, R. L. Cheu, Competitive facility location on decentralized supply chains, European Journal of Operational Research vol. 196 pp. 487–499, 2009.

[17] V. M. Trenkel, M. J. Rochet, Intersection–union tests for characterising recent changes in smoothed indicator time series, ecological indicators vol. 9 pp. 732 –739, 2009.

[18] J. Kim, Identification of lateral tyre force dynamics using an extended Kalman filter from experimental road test data, Control Engineering Practice vol. 17 pp. 357–367, 2009.

[19] T. Schneidera, J. M. Fielkeb, Simulating the cornering behaviour of multiple trailed implements, Biosystems Engineering vol. 100 pp. 355-361,2008.

[20] F. Braghin, F. Cheli, S. Melzi, E. Sabbioni, Race driver model, Computers and Structures vol. 86 pp. 1503–1516,2008.

[21] J. Ste´phanta, A. Chararaa, D. Meizel, Evaluation of a sliding mode observer for vehicle sideslip angle, Control Engineering Practice vol. 15 pp. 803–812,2007.

[22] N. L. Blacka, B. Dasb, A three-dimensional computerized isometric strength measurement system, Applied Ergonomics vol. 38 pp. 285–292,2007.

[23] L. H.V. van der Woude, S. d. Groot,T. W. J. Janssen, Manual wheelchairs: Research and innovation in rehabilitation, sports, daily life and health, Medical Engineering & Physics vol. 28 pp. 905–915, 2006.

[24] S. Kalyanasundaram, A. Lowe, A. J. Watters, Finite element analysis and optimization of composite wheelchair wheels, Composite Structures vol. 75 pp. 393–399, 2006.

[25] P. B. U. Andersson, W. Kropp, Rapid tyre/road separation: An experimental study of adherence forces and noise generation, Wear vol. 266 pp. 129–138, 2009.